doi:10.1016/j.jmb.2005.07.016 J. Mol. Biol. (2005) 352, 165–177

JMB

Available online at www.sciencedirect.com

SCIENCE DIRECT®

ELSEVIER

Structural Insights into Drug Processing by Human Carboxylesterase 1: Tamoxifen, Mevastatin, and Inhibition by Benzil

Christopher D. Fleming[1,2], Sompop Bencharit[1,3], Carol C. Edwards[4] Janice L. Hyatt[4], Lyudmila Tsurkan[4], Feng Bai[5], Charles Fraga[5] Christopher L. Morton[4], Escher L. Howard-Williams[1], Philip M. Potter[4] and Matthew R. Redinbo[1,2,6]*

[1]*Department of Chemistry University of North Carolina at Chapel Hill, Chapel Hill, NC 27599, USA*

[2]*Department of Biochemistry and Biophysics, University of North Carolina at Chapel Hill Chapel Hill, NC 27599, USA*

[3]*School of Dentistry, University of North Carolina at Chapel Hill Chapel Hill, NC 27599, USA*

[6]*Lineberger Comprehensive Cancer Center, University of North Carolina at Chapel Hill Chapel Hill, NC 27599, USA*

[4]*Department of Molecular Pharmacology, St. Jude Children's Research Hospital Memphis, TN 38105, USA*

[5]*Department of Pharmaceutical Sciences, St. Jude Children's Research Hospital, Memphis TN 38105, USA*

**Corresponding author*

Human carboxylesterase 1 (hCE1) exhibits broad substrate specificity and is involved in xenobiotic processing and endobiotic metabolism. We present and analyze crystal structures of hCE1 in complexes with the cholesterol-lowering drug mevastatin, the breast cancer drug tamoxifen, the fatty acyl ethyl ester (FAEE) analogue ethyl acetate, and the novel hCE1 inhibitor benzil. We find that mevastatin does not appear to be a substrate for hCE1, and instead acts as a partially non-competitive inhibitor of the enzyme. Similarly, we show that tamoxifen is a low micromolar, partially non-competitive inhibitor of hCE1. Further, we describe the structural basis for the inhibition of hCE1 by the nanomolar-affinity dione benzil, which acts by forming both covalent and non-covalent complexes with the enzyme. Our results provide detailed insights into the catalytic and non-catalytic processing of small molecules by hCE1, and suggest that the efficacy of clinical drugs may be modulated by targeted hCE1 inhibitors.

Keywords: drug metabolism; protein structure; X-ray crystallography; therapeutic design; glycoprotein

Introduction

Human carboxylesterase 1 (hCE1) is a broad-spectrum serine hydrolase (EC 3.1.1.1) that cleaves small ester, thioester, and amide ester linkages in a variety of structurally distinct compounds.[1] The enzyme is present in numerous tissues, including heart, intestines, kidney, lung, testes, monocytes and macrophages, but is expressed most abundantly in the liver, where it plays a major role in the detoxification of potentially harmful xenobiotics and endobiotics.[2,3] hCE1 is known to metabolize a

Abbreviations used: hCE1, human carboxylesterase 1; rCE, rabbit liver carboxylesterase; HMG-CoA, 3-hydroxy-3-methylglutaryl coenzyme A; ACAT, acyl-coenzyme A cholesterol acyltransferase; CE, carboxylesterase; CEH, cholesterol ester hydrolase; FAEE, fatty acyl ethyl esters; CNS, crystallography and nuclear magnetic resonance software; NAG, *N*-acetylglucosamine; SIA, sialic acid; EA, ethyl acetate; NCP, non covalent product; COV, covalent product; PEG, polyethylene glycol.

E-mail address of the corresponding author: redinbo@unc.edu

0022-2836/$ - see front matter

variety of drugs, including cocaine, meperidine, and lidocaine,[4–6] and to activate a variety of prodrugs, including heroin, the chemotherapeutic capecitabine, and the angiotensin-converting enzyme inhibitors temocapril, imidipril, and delapril.[6–8] The enzyme utilizes a two-step serine hydrolase mechanism involving the formation of a covalent acyl-intermediate on the active site serine residue, which is subsequently removed by hydrolysis. In addition, the enzyme is able to perform transesterification reactions to generate secondary metabolites of abundant endogenous and xenobiotic compounds.[9,10]

Three crystal structures of hCE1 and one structure of a rabbit liver CE (rCE) have been reported to date.[11–13] hCE1 exists in a trimer–hexamer equilibrium,[12] and the overall structure of the hCE1 trimer is shown in Figure 1(a). Each monomer is comprised of a catalytic domain, an α/β domain typical of hydrolases, and a regulatory domain that contains the low-affinity surface ligand-binding Z-site.[11,12] The regulatory domain was identified in the first crystal structure of a mammalian CE (that of rCE, which shares 81% sequence identity and 0.68 Å rmsd with hCE1),[12] and was so-termed because it was proposed to regulate access to the catalytic gorge.[13] The active site of the enzyme containing the catalytic triad Ser221-His468-Glu354 is a 10–15 Å deep hydrophobic pocket at the interface of the three domains. A secondary pore into the active site of mammalian CEs, termed the side door, has been proposed on the basis of the observed binding of a product of the activation of the anticancer drug CPT-11 to rCE.[13] Each hCE1 monomer also contains two disulfide linkages and one high-mannose, N-linked glycosylation site on Asn79, where only the first *N*-acetylglucosamine (NAG) and terminal sialic acid (SIA) molecules could be placed properly in the electron density maps for all complexes. A surface ligand-binding site (the above-mentioned Z-site) was found to control the trimer–hexamer equilibrium of hCE1; this site has been observed either to contain bound ligand, or to be involved in the formation of the hCE1 hexamer.[12]

The statins, currently some of the most widely prescribed drugs in the USA, lower serum cholesterol levels by inhibiting 3-hydroxy-3-methylglutaryl-coenzyme A (HMG-CoA) reductase, which catalyzes the rate-limiting step in cholesterol biosynthesis.[14] Mevastatin (Compactin), a class 1 statin similar to simvastatin (Zocor®, Merck) and lovastatin (Mevacor®, Merck), is believed to be activated by hCE1 in the liver by conversion of the lactone form of the drug to the carboxylate form.[5,15] Newer class 2 statins, such as rosuvastatin (Crestor®, AstraZeneca) and atorvastatin (Lipitor®, Pfizer), already exist in the carboxylate form, which removes the requirement for activation.[16] Although mevastatin was never used clinically, it provided the basis for the development of this family of drugs,[14] and provides an effective model to examine the potential activation of clinical drugs by hCE1.

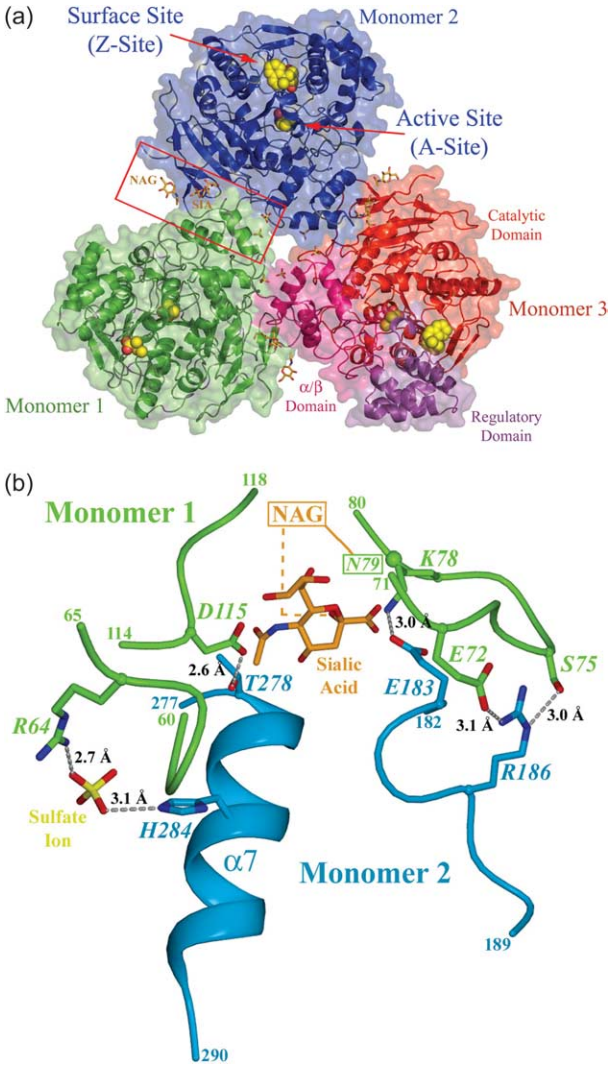

Figure 1. Trimeric structure of hCE1. (a) Overall structure of hCE1 in complex with mevastatin. Sulfate group are indicated in yellow, carbohydrates are shown in orange, and mevastatin products are depicted as yellow and red space-filling models. Monomer 3 is colored separately by domain with the catalytic domain in red, the α/β domain in pink, and the regulatory domain in magenta. (b) Expanded view of the trimer interface indicated by a box in (a). The distances (in Å) are represented by black dotted lines, with the gold dotted line representing the high-mannose glycosylation chain between the initial *N*-acetylglucosamine (NAG) and the terminal sialic acid molecule.

Tamoxifen, a non-steroidal estrogen receptor antagonist used to treat breast cancer, limits the estrogen-dependent proliferation of cancerous cells.[17] It is the most widely used anticancer drug in the world,[18] and the ability of this compound to pass successfully through the liver is central to its efficacy.[19] hCE1 was not thought to be involved in the trafficking of tamoxifen through the body until it was found that only four proteins in rat liver bound a labeled form of tamoxifen, and one of these proteins was the rat homologue of hCE1.[20] Thus, it

is possible that the binding of tamoxifen to hCE1 may limit the bioavailability of the drug, or may lead to drug–drug interactions and/or side-effects associated with tamoxifen use, including impact on cholesterol levels.[21]

In addition to its role in xenobiotic metabolism, hCE1 has been shown to catalyze reactions involved in cholesterol homeostasis and fatty acid metabolism. For example, hCE1 has been reported to possess acyl-coenzyme A:cholesterol acyltransferase (ACAT) activity, which generates cholesterol esters from fatty-acyl coenzyme A and free cholesterol.[22] hCE1 has also been found to catalyze the reverse reaction under certain conditions and in that way to act as a cholesterol ester hydrolase (CEH).[23] In addition, the enzyme can produce fatty acyl ethyl esters (FAEEs) *via* the transesterification of short-chain and long-chain fatty acids with ethanol.[24] FAEEs are toxic byproducts associated with long-term alcohol abuse, and these compounds have been implicated in the necrotic decay of the liver and other tissues attendant with such abuse.[25] The FAEEs generated by the FAEE synthases disrupt cellular function by uncoupling oxidative phosphorylation in the inner membrane of mitochondria.[26,27] There are four enzymes known to act as FAEE synthases, with hCE1 labeled as FAEE-synthase IV.[25,28]

The novel and potent hCE1-selective inhibitor benzil was identified during screens to discover compounds that would inhibit CE activity to aid in anticancer drug efficacy. The diphenyl-diketone compound benzil was found to inhibit hCE1-mediated hydrolysis of *o*-nitrophenyl acetate with a K_i value of 45 nM.[29] It was not clear, however, whether this compound functioned by binding non-covalently or covalently to the active site of hCE1.

We sought to examine at the structural level how hCE1 processes a variety of therapeutic and non-therapeutic compounds. To that end, we determined crystal structures of hCE1 in complexes with mevastatin, tamoxifen, ethyl acetate (a fatty acyl ethyl ester analogue), and benzil, and we examined the inhibitory action of mevastatin and tamoxifen on the enzyme. Our results suggest that certain classes of compounds are capable of inhibiting this drug metabolism enzyme, and that selective inhibitors of hCE1 may impact the bioavailability of clinical drugs.

Results

Structural features of hCE1

The hCE1–ligand complex crystal structures reported here were refined with the Crystallography and NMR System (CNS),[30] utilizing torsion angle dynamics throughout all steps, and with simulated annealing and non-crystallographic symmetry restraints in the early steps of refinement (Table 1). Despite relatively high R_{sym} values for the diffraction data employed, the maps produced after

Table 1. Crystallographic statistics

	Mevastatin	Ethyl acetate	Tamoxifen	Benzil
Resolution (Å)[a]	50–3.0 (3.11–3.0)	50–3.0 (3.2–3.0)	50–3.2 (3.31–3.2)	50–3.2 (3.31–3.2)
Space group	$P2_12_12_1$	$P2_12_12_1$	$P2_12_12_1$	P1
Asymmetric unit	One trimer	One trimer	One trimer	Four trimers
Cell constants				
a (Å)	55.78	55.50	55.37	54.56
b (Å)	181.59	181.15	179.59	181.49
c (Å)	202.87	203.01	201.58	202.71
α (deg.)	90	90	90	90.12
β (deg.)	90	90	90	89.93
γ (deg.)	90	90	90	89.72
Total reflections	462,117	289,419	690,386	681, 289
Unique reflections	42,843	41,952	34,502	125, 020
Mean redundancy	10.8	6.9	20.0	5.5
R_{sym} (%)[a,b]	12.8 (41.5)	13.5 (46.7)	13.5 (32.6)	15.6 (44.6)
Wilson *B*-factor (Å^2)	29.7	45.3	37.3	32.2
Completeness[a] (%)	98.1 (97.5)	99.7 (98.6)	98.5 (99.6)	97.2 (96.9)
Mean I/σ[a]	11.3 (3.7)	10.5 (2.1)	7.0 (2.2)	3.9 (1.8)
R_{cryst}[c] (%)	18.7	19.0	20.3	20.7
R_{free}[d] (%)	24.7	22.9	25.2	28.7
Number of atoms:				
Protein	12,391	12,390	12,385	50,078
Solvent	347	420	193	468
Carbohydrate	105	105	105	420
Ligand	74	36	168	227
Ion	30	30	30	120

[a] Numbers in parentheses are for the highest shell.
[b] $R_{sym} = \Sigma|I - \langle I \rangle|/\Sigma I$, where I is the observed intensity and $<I>$ is the average intensity of multiple symmetry-related observations of that reflection.
[c] $R_{cryst} = \Sigma||F_o| - |F_c||/\Sigma|F_o|$, where F_o and F_c are the observed and calculated structure factors, respectively.
[d] $R_{free} = \Sigma||F_o| - |F_c||/\Sigma|F_o|$ for 7% of the data not used at any stage of structural refinement.

refinement were of good quality and allowed the placement of both protein and non-protein atoms. The asymmetric unit of the mevastatin, ethyl acetate, and tamoxifen complexes contained one hCE1 trimer, while the asymmetric unit of the benzil complex contained four hCE1 trimers.

Because a detailed examination of the trimer interfaces in CEs had not been reported, an analysis of the role of carbohydrate groups in the formation of the hCE1 trimer is presented here. A sialic acid from the glycosylation site on one monomer stacks adjacent to α7 and Glu183 in the adjacent monomer within the trimer (Figure 1(b)). In some cases, the sialic acid molecule is within 3 Å of the main-chain nitrogen atom at Thr279, which appears to stabilize the N-terminal, positively charged dipole of helix α7. There are two charge clamps across the trimer interface, Arg186 and Glu183 of one monomer to Glu72 and Lys78, respectively, of the next monomer. Six bound sulfate groups near His284 are observed. While the monomers within the hCE1 trimer are related by non-crystallographic symmetry, the monomers in the structure of the related rabbit enzyme rCE (RCSB PDB accession code 1KY4)[13] form a trimer related by crystallographic symmetry. In this case, although rCE also contains a similar glycosylation site at Asn79, a carbohydrate group does not appear to be involved in the rCE trimer interface. This N-linked carbohydrate is important for enzyme function, however, as the mutation of Asn79 to alanine in rCE reduces esterase activity by ~50% using *o*-nitrophenol acetate as a substrate (M. Espinosa and P.M.P., unpublished results). An alignment of several mammalian CEs (from mouse, rat, rabbit, human, guinea pig, pig, and monkey) revealed that residues involved in the trimer interface observed in hCE1 and rCE are identical or conserved across species.[31] In addition, both rat and porcine CE isoforms related in sequence to hCE1 have been shown biochemically to form trimers.[32–34] Thus, the known mammalian homologues of hCE1 appear to be trimers.

Drug processing: mevastatin

Since previous reports in the literature implicated hCE1 in the activation of Mevastatin,[5,14,35] we sought to determine the structural basis for this hydrolysis event. hCE1 is potentially capable of metabolizing mevastatin *via* two pathways (Figure 2(a)): α-cleavage opens the lactone ring, yielding the active, carboxylate form of the drug; β-cleavage, the alternative pathway, involves the removal of an isopentoic acid (2-methylbutyric acid) moiety from the compound, reducing the inhibitory effect of the drug on HMG-CoA reductase by 200-fold.[36–38] We crystallized the enzyme in the presence of 100-fold molar excess mevastatin, and determined and refined the structure to 3.0 Å resolution. While the α-cleavage product was expected, the initial 3.0 σ positive difference electron density in the active sites was too small to accommodate the α-cleavage product. However, simulated annealing omit electron contoured at 3.0 σ appeared appropriate for an isopentoic acid, the small product of mevastatin β-cleavage (Figure 2(b)). Isopentoic acid refined well in this position, produced no negative electron density, and forms a hydrogen bond between one of its carboxylate oxygen atoms and a water molecule bound within the oxyanion hole of the enzyme.

We also observed 3.0 σ positive difference density within the Z-site of each monomer, the non-specific, low-affinity cleft that can be occupied by a wide variety of structurally distinct ligands.[11,12] The Z-site is formed by two loops, Ω1 and Ω2, which interdigitate during hexamer formation, providing primary stacking interactions between the two trimers.[12] In one Z-site within the trimer, the difference density was appropriate for an isopentoic acid stabilized *via* an electrostatic contact between its carboxylate group and the ζ nitrogen atom of Lys414. In the remaining two monomers, the electron density was interpreted to be the other product of mevastatin β-cleavage (the larger, decalin-lactone alcohol; Figure 2(c)); this compound refined well in this position and produced no negative electron density. It docks with its lactone ring facing down in van der Waals contact with Leu368 and Trp357, and forms a hydrogen bond with Lys414. The α-cleavage product of mevastatin, in contrast, did not satisfy this electron density at the Z-site.

Because the crystallographic data indicated the presence of β-cleavage products bound to hCE1, we sought to validate our results biochemically utilizing an HPLC-based *in vitro* assay. After a 25 day incubation of purified hCE1 with tenfold molar excess mevastatin at 37 °C in 50 mM Hepes (pH 7.4) (the conditions used for crystallization of this complex), we were unable to detect enzyme-mediated production of either the α-cleavage or β-cleavage products (data not shown). Since these results were contrary to what we observed structurally, we assessed whether mevastatin could act as an inhibitor towards hCE1. These experiments confirmed that the drug was a weak, partially non-competitive inhibitor of *o*-nitrophenyl acetate hydrolysis by hCE1 with a K_i value of 20.8(±8.8) μM. Previous studies have shown that similar statins (lovastatin, simvastatin) are able to inhibit human butyrylcholinesterase, a structural homologue of hCE1, with K_i values of the same order as that observed for hCE1 inhibition by mevastatin (12 μM for lovastatin and 4.5 μM for simvastatin).[39] Thus, mevastatin appears to act *in vitro* as a weak inhibitior of hCE1.

Substrate conjugation: FAEEs

Fatty acyl ethyl esters (FAEEs), toxic byproducts of alcohol abuse, are generated by hCE1 *via* the transesterification of fatty acids with ethanol.[24] To elucidate the structural basis of the action of hCE1 as an FAEE synthase, we attempted to crystallize the enzyme in the presence of ethanol and one of a

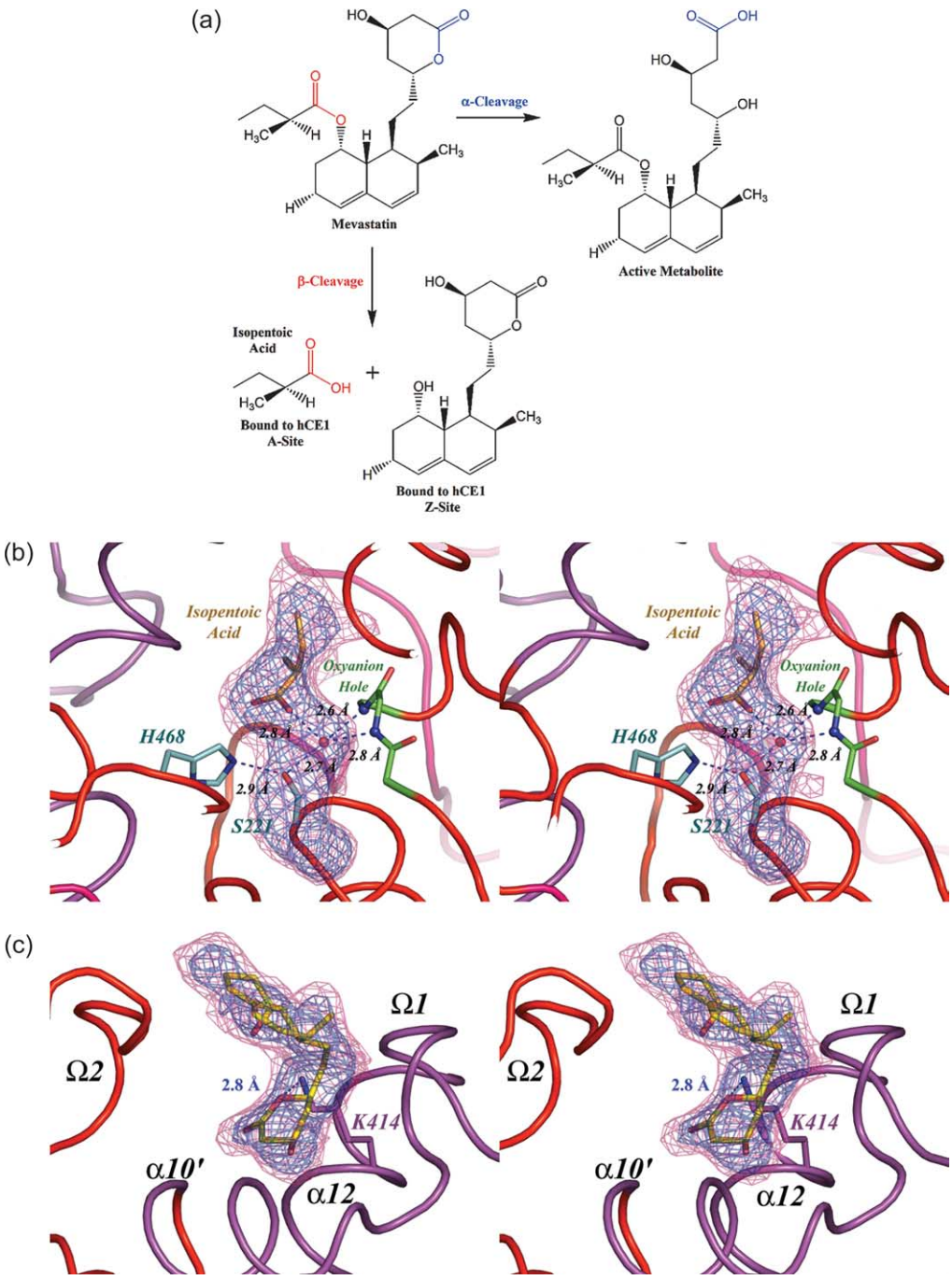

Figure 2. Mevastatin metabolism by hCE1. (a) Potential mechanisms of mevastatin cleavage by hCE1. The locations of the α and β-cleavage sites are shown in blue and red, respectively. (b) Stereo view of the active site of hCE1 showing the isopentoic acid product of mevastatin β-cleavage (gold) bound to the catalytic residues. Simulated annealing omit maps, at 3.0 Å resolution, are contoured to 3.0 σ (blue) and 2.0 σ (magenta). Ser221 and His468 are shown in cyan, with the catalytic water molecule in red. The oxyanion hole is represented in stick format (green), and all distances are displayed as blue dotted lines. (b) and (c) Protein secondary structure is colored by domain according to Figure 1(a), monomer 3. (c) The β-cleavage decalin product of mevastatin bound to the non-specific Z-site of hCE1. Simulated annealing omit maps are shown as in (b). The hydrogen bonding main-chain carbonyl groups are shown in green. Water-mediated hydrogen bonding is represented as blue lines.

variety of poorly soluble fatty acids and related compounds. Crystals were obtained only in the presence of ethanol and acetyl-CoA, the most soluble of the compounds tested. We found that hCE1 had transesterified acetyl-CoA with ethanol to form ethyl acetate (EA), a small FAEE mimic (Figure 3(a)). Strong electron density for EA was observed in 3.0 Å simulated annealing omit maps at both the active site and Z-site of the enzyme (Figure 3(b)). The EA bound at the active site forms van der Waals contacts with only two amino acid residues within the pocket, Ser221 and Leu304, and

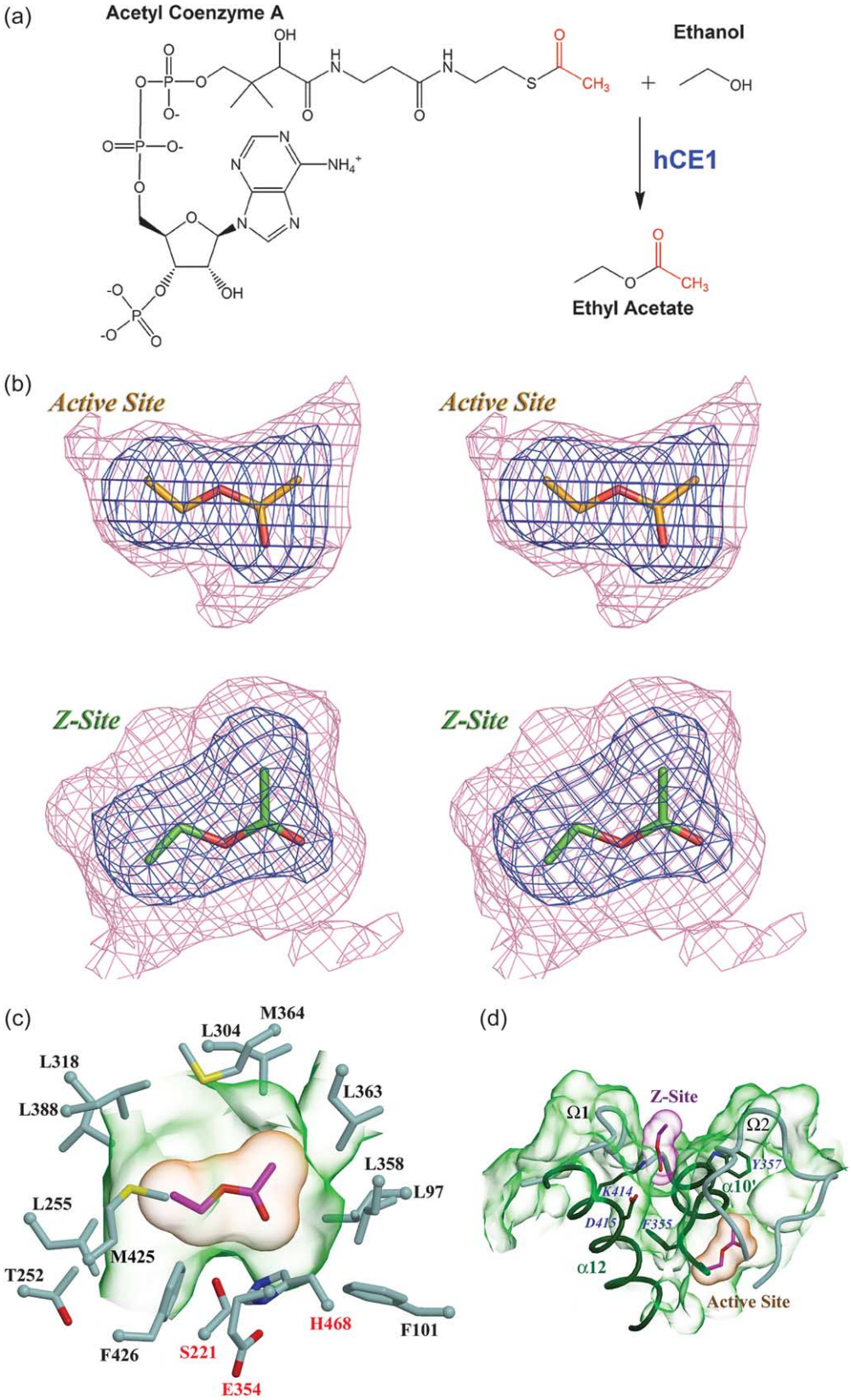

Figure 3. FAEE-type conjugation by hCE1. (a) Mechanism of hCE1-dependent ethyl acetate (EA) production by transesterification of acetyl-CoA with ethanol. The transferred acetyl group is indicated in red. (b) Stereo view of 3.0 Å simulated annealing omit maps of EA bound at both active and Z-sites. Maps are contoured to 4.0 σ and 2.0 σ (blue and magenta, respectively) for the active site with 6.0 σ and 2.0 σ (blue and magenta, respectively) for the Z-site. (c) EA bound to the active site of hCE1. The molecular surface of the hCE1 active site cavity is represented in green, with the catalytic triad labeled in red. (d) EA bound to the Z-site, located slightly above the EA bound within the active site. The molecular surface of the protein is represented in green, with the Ω loops shown in grey, and the helices in dark green.

thus does not appear to bind with a high level of specificity (Figure 3(c)). Non-specific binding is observed at the Z-site, where EA forms only a hydrogen bond with Lys414 (Figure 3(d)). These data indicate that hCE1 can accommodate acetyl-CoA within its active site and utilize ethanol to transesterify the acetyl product of acetyl-CoA cleavage to generate EA.

Drug binding: tamoxifen

The rat homologue of hCE1 (ES-10) was found to be one of only four liver proteins that bound to tamoxifen with high affinity.[20] We sought to elucidate the structural basis of the ability of hCE1 to interact with this widely used anticancer drug, and to determine if tamoxifen inhibited the enzyme. Tamoxifen was observed bound at both the active site and Z-site in our 3.2 Å structure of the drug-hCE1 complex (Figure 4(a)). Tamoxifen is well ordered within the catalytic pocket, making hydrophobic contacts with eight active site residues that line the pocket (Figure 4(b)). Indeed, tamoxifen's triphenyl structure fits remarkably well in the binding cavity, with two of the rings filling pockets adjacent to Phe101 and Leu388, and the tail of the drug protruding toward the entrance to the cavity. Leu304, which sits near the top of the pocket, undergoes a rotamer shift relative to other hCE1 structures to provide room for drug binding. Helices α1 and α10′ clamp over the top of the active site, closing down onto the tamoxifen compound. It has been proposed that α10′ has the ability to shift in position to allow bulky molecules to enter the active site (Figure 4(c)).[12] Once the position of α10′ becomes relatively stable, it serves as the "floor" of the Z-site. Tamoxifen binds with less specificity at the Z-site, making only four van der Waals contacts with amino acid side-chains and exhibits higher thermal displacement parameters in this position (69–79 $Å^2$) relative to that observed at the active site (30–43 $Å^2$).

We found that tamoxifen was a micromolar affinity inhibitor of both hCE1 and rCE, with K_i values of 15.2(±2.8) and 23.3(±14.3) μM, respectively. The K_i values agree with previous work showing tamoxifen as a CE inhibitor in rat.[20] We found also that both hCE1 and rCE are inhibited by tamoxifen in a partially non-competitive fashion. In the case of hCE1, these results indicate that the

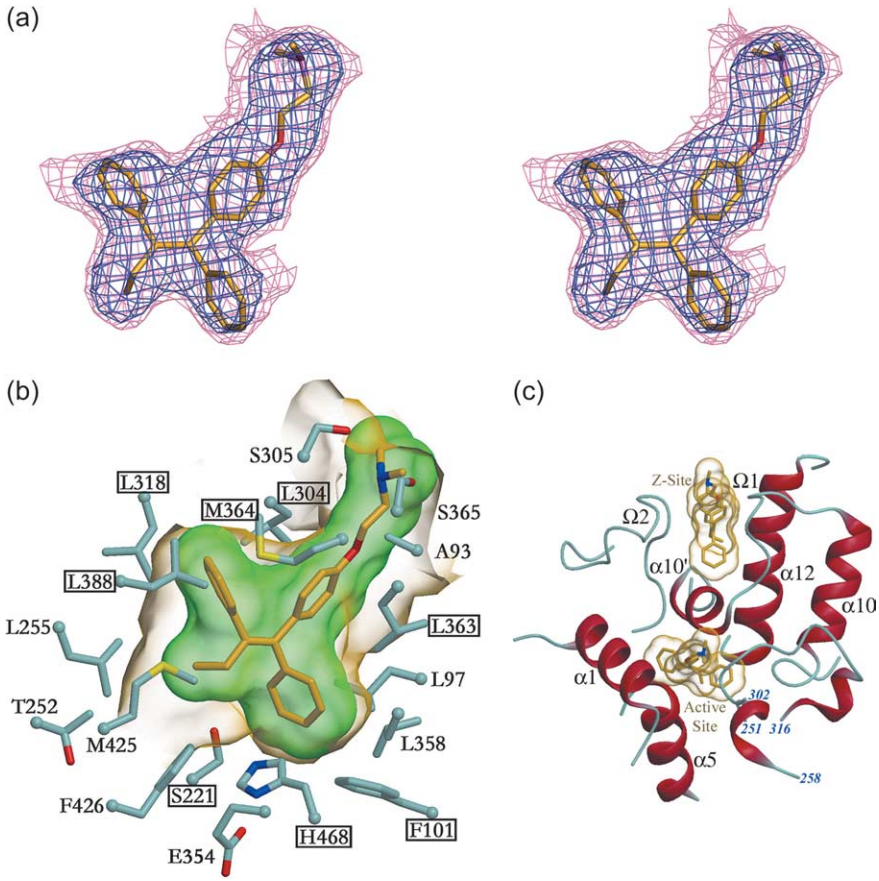

Figure 4. Binding of tamoxifen by hCE1. (a) Stereo view of simulated annealing omit map of tamoxifen (gold) bound to the active site of hCE1. Maps are at 3.2 Å resolution and contoured to 3.0 σ (blue) and 2.0 σ (magenta). (b) Tamoxifen bound within the active site gorge. The molecular surface of tamoxifen (green) and the surface of the hCE1 active site (gold) indicate that the drug fits in a complementary manner. Amino acid residues making hydrophobic contacts with tamoxifen are boxed in black. (c) Relationship of the active site to the Z-site in the hCE1–tamoxifen complex. The secondary structure is labeled and tamoxifen is shown in gold.

Z-site may act as an allosteric site. The Z-site is located directly "above" the active site, separated from it by α10′ (Figure 4(c)), and may control ligand access to the active site.[12] The analogous loops are disordered in the rCE structure, so it is not known whether this enzyme contains a surface Z-site. A surface binding site proposed to act in a similar manner, as an allosteric or substrate recognition site, was observed recently in the structure of the human drug metabolism enzyme cytochrome P450-3A4.[40]

Inhibition of hCE1: benzil

Finally, we determined the crystal structure of hCE1 in complex with benzil, a potent CE inhibitor with a K_i value of 45 nM for hCE1.[29] The structure contained four trimers in the P1 asymmetric unit, which will be referred to as trimers A–D, with each monomer denoted 1–3 (e.g. monomer A3 or D1). Positive (2.0–3.0 σ) difference density in the active site in all 12 monomers was not satisfied by placement of intact benzil. After further examination and refinement, it appeared that hCE1 had cleaved benzil to generate a covalent product and either benzaldehyde and/or benzoic acid. On the basis of our structural results, we propose that the following elements may be involved in benzil inhibition of hCE1 (Figure 5(a)). First, a cycling reaction may occur in which attack of the catalytic Ser221 residue on one of the carbonyl groups of benzil to form the covalent intermediate reverses to generate benzil and free enzyme (Figure 5(a)). Such a repeating cycle would occupy the active site and inhibit the enzyme efficiently. This is consistent with the previously published kinetic analyses.[29]

Second, benzil could be hydrolyzed to the two benzyl ring products we have named NCP1 (benzaldehyde, or non-covalent product 1) and NCP2 (benzoic acid). Such a cleavage reaction would require a retro-aldol condensation followed by a hydrolysis event (Figure 5(a)). For formation of benzaldehyde, a transfer of electrons from the first hydroxyl group to the second carbonyl carbon atom would occur, releasing NCP1. This movement of electrons would also result in the covalent acyl product found in three of the active sites (COV). A hydrolysis event, analogous to the second step of the standard two-step serine hydrolase mechanism, would then be required to remove the benzoyl ester intermediate and release the second benzyl ring product benzoic acid (NCP2), as well as the free enzyme (Figure 5(a)). Of the 12 monomers in the asymmetric unit, three of the active sites contain the covalent modification, (A3, B3, and D1) and the remaining nine contain the NCP products. In one of the monomers that contains the covalent modification (A3; Figure 5(b)), the free carboxylic oxygen atom is within hydrogen bonding distance of the oxyanion hole, and replaces a water molecule typically observed in that position (see Figure 2(b)).

Analysis of hCE1 by mass spectrometry was attempted to detect covalently bound product, but was not successful due to our inability to remove the high-mannose glycosylation sites using the enzymes PNGase F and/or Endo-F1; these efforts produced extensive mass-charge heterogeneity (data not shown). Simulated-annealing omit difference density maps, however, indicate the presence of covalent modification and of non-covalent product (NCP) binding (Figure 5(d)). This is the first structure of hCE1 in which the enzyme is observed to be covalently modified. Benzoic acid (NCP) binding is similar to other smaller ligands, including the isopentoic acid product of mevastatin (Figure 5(c); see also Figure 2(b)). It is held in place primarily by a direct hydrogen bond to a water molecule, which exhibits clear tetrahedral geometry in the oxyanion hole. This geometry is similar to that seen for the free carboxylic oxygen atom in the covalent product (see Figure 5(b)). NCP products are found also in all 12 Z-sites with binding modalities similar to non-specific binding seen in other hCE1 complexes. The observation of covalent and non-covalent complexes at the hCE1 active site helps to explain how the dione structure of benzil inhibits hCE1, and may provide an avenue to design more effective hCE1 inhibitors for clinical use.

Discussion

Mevastatin

Analysis of hCE1 crystallized in the presence of mevastatin indicated that isopentoic acid was present within the active site of the protein. Because we assumed that mevastatin would be a substrate for CEs,[5,15] we hypothesized that the observed isopentoic acid resulted from hCE1-mediated β-activation of the drug (Figure 2(a)–(c); the other product of this activation would be a decalin-lactone compound). At the Z-site, electron density was interpreted as the decalin-lactone compound, although it is possible that the product of α-activation may be present also (Figure 2(a) and (c)). *In vitro* biochemical assays using purified hCE1 and mevastatin as a substrate failed to detect the presence of isopentoic acid or the larger, decalin-lactone alcohol product. Subsequent analyses indicated that mevastatin was a partially non-competitive inhibitor of hCE1. The inhibition of hCE1 occurs at moderately low concentrations of mevastatin (~20 μM), which may have biological consequences. Thus, it is possible that hCE1 does not activate mevastatin *in vivo*. Human serum paraoxonase (PON1) may instead perform this catalytic processing, as it has been shown to contain lactonase activity toward the statin class of compounds.[41]

It is possible that the complexes of hCE1 with portions of mevastatin that we observe in our structure arose from a mechanism similar to that seen with benzil, i.e. that under prolonged incubation of enzyme with drug, very low levels of

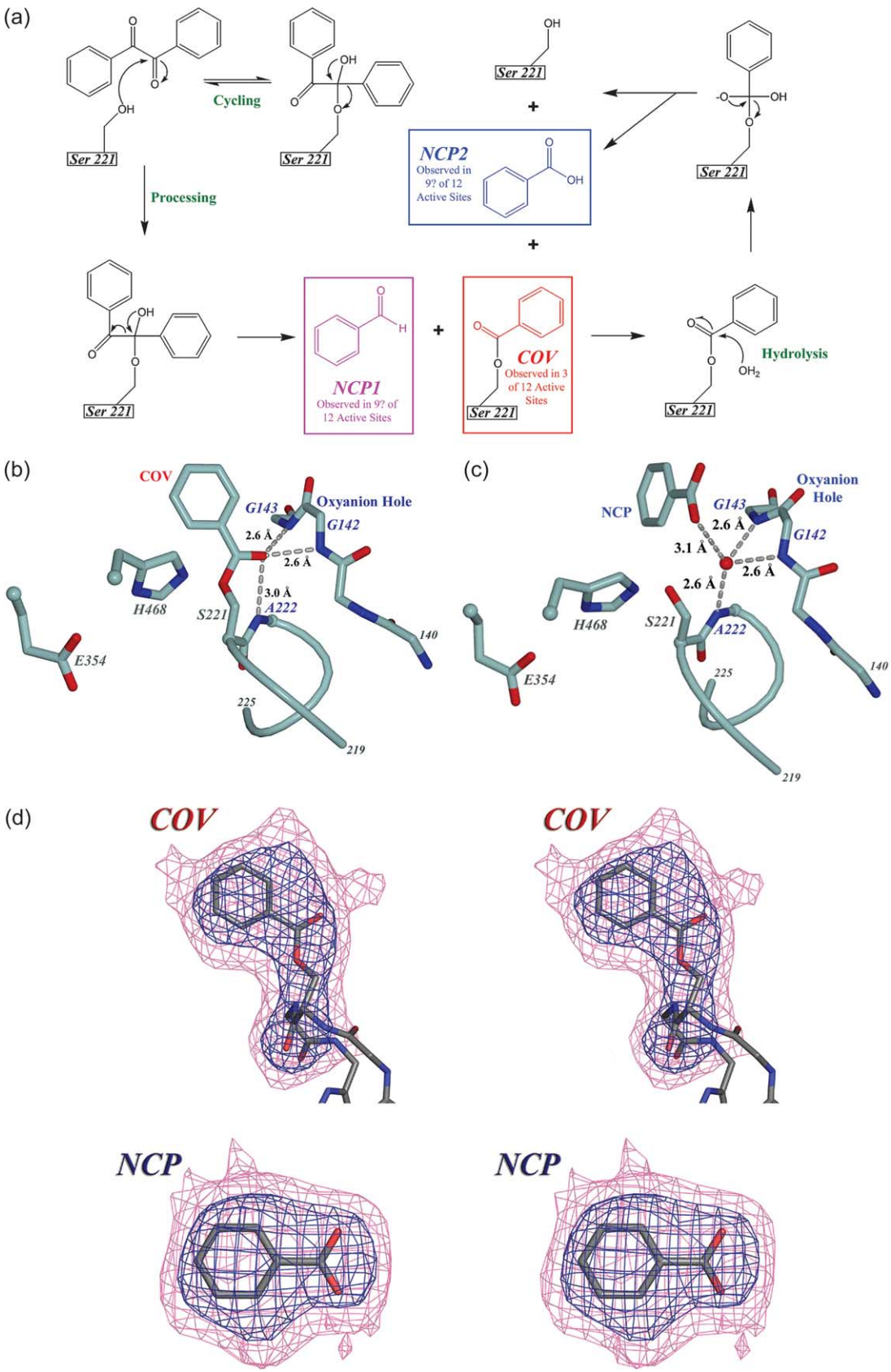

Figure 5. hCE1 inhibition by benzil. (a) Proposed mechanism of benzil inhibition and processing by hCE1. Non covalent products NCP1 (benzaldehyde, in purple) or NCP2, (benzoic acid, in blue) are found in nine out of 12 active sites, with the covalent product (COV) found in three of 12 active sites, depicted in red. (b) Covalent modification of the catalytic serine residue by benzil. The catalytic triad is labeled in grey with the oxyanion hole in blue. (c) NCP2 bound to the active site of hCE1. The catalytic water molecule is represented as a red sphere and amino acid residues are labeled as in (b). (d) Stereo views of the simulated annealing omit maps at 3.2 Å resolution of the active site COV and NCP2 complexed with hCE1, contoured to 2.0 σ (magenta) and 4.0 σ (blue).

hydrolysis may occur, resulting in the generation of a small molecule (isopentoic acid for mevastatin) that stabilizes protein structure. This would favor formation of the crystal containing this moiety and hence may "select" this structure due to increased thermodynamic stability. We would expect that crystallization trials with isopentoic acid (2-methyl-butyric acid) alone would give similar results. It is possible, however, that hCE1 does play a role *in vivo* in mevastatin activation, but that our *in vitro* conditions failed to reproduce the conditions found in human tissues that enable catalytic action. For example, the processing of mevastatin by hCE1 may require the presence of other proteins necessary to traffic the substrate into or the products away from the active site of the enzyme.

Production of ethyl acetate

The mechanism of transesterification of acetyl CoA with ethanol to form EA is likely a simple modification of the standard two-step serine hydrolase mechanism, with ethanol replacing water in second step that releases the bound acyl-enzyme intermediate. An open question, however, is how ethanol gains access to this intermediate, which is formed from the cleavage of the thioester bond in acetyl CoA (Figure 3(a)). Acetyl CoA fills the active site cavity of hCE1 (S.B. *et al.*, unpublished results). Thus, we suggest that ethanol accesses the active site gorge *via* the side door secondary pore first identified for the mammalian carboxylesterases in the structure of a rabbit liver CE (rCE).[13] This pore, which lies adjacent to Thr252 at the base of the active site gorge, appears capable of allowing ethanol or water to enter the active site without having to negotiate past the bound CoA molecule. We have seen that this pore is used by the enzyme to allow long fatty acyl regions of endogenous hCE1 substrates to extrude from the active site of the enzyme (S.B. *et al.*, unpublished results). Thus, the catalytic action of hCE1 on a variety of structurally distinct substrates appears to be enhanced by the presence of an additional channel into and out of the active site of the enzyme, which enables larger and more varied substrate molecules access to the buried catalytic residues.

Sequestering of tamoxifen

The binding of tamoxifen to hCE1 could affect the efficacy of this chemotherapeutic agent. The drug is administered in 20 mg doses once or twice daily and, upon trafficking through the liver, a fraction of it likely binds to hCE1. This may delay the passage of the drug out of the liver, or enhance its clearance by other hepatic enzymes. The use of selective inhibitors of hCE1 could improve tamoxifen efficacy by blocking tamoxifen binding by the enzyme. The non-productive binding of tamoxifen to hCE1 could also contribute to the side-effects of the drug. hCE1 has been reported to contain both cholesterol ester hydrolase (CEH) and acyl-CoA cholesterol transferase activities (ACAT),[22,23] and thus even weak inhibition of hCE1 by tamoxifen could impact cholesterol metabolism.[42]

Degradation of benzil

It was not possible to distinguish between the two NCP products of benzil hydrolysis in our 3.2 Å resolution crystal structure. By electron density considerations alone, two orientations of benzaldehyde (NCP1) could appear to be a benzoic acid molecule (NCP2). Thus, we conclude that either NCP1 or NCP2 could be present in the nine enzyme active sites where no covalent modification is observed (Figure 5(a)). We chose to place benzoic acid (NCP2) in the active sites because this single molecule satisfied the electron density; however, multiple orientations of small planar molecules are possible and have been seen in other hCE1-ligand structures.[11] The presence of these NCP products within the active site of hCE1 likely results from the extended time-frame required for crystal growth (two months). Indeed, similar to the structures derived from the mevastatin incubations described above, the crystallization of the hCE1–benzil complex appears to require the stabilizing effects of these small ligand products of slow substrate hydrolysis events.

Overall, these studies provide insights into the mechanism of hCE1, and into inhibition of the enzyme by a variety of molecules. Our results indicate that esters can act either as substrates or as inhibitors for hCE1; thus, predicting whether a compound will be hydrolyzed by the enzyme is difficult. In addition, our studies suggest that the use of hCE1 inhibitors of CEs could modulate drug disposition *in vivo*, as has been achieved successfully in the clinics with inhibitors of other drug metabolism enzymes.[43]

Experimental Procedures

Crystallization and crystal handling

A secreted form of hCE1 was expressed using baculovirus in *Spodptera frugiperda* Sf21 cells and purified as described.[44,45] All ligands were purchased from Sigma. hCE1 was concentrated to 8–10 mg ml^{-1} in 50 mM Hepes (pH 7.4) and kept at 4 °C prior to crystallization. Since the solubility of the ligands varied, different methods were utilized for crystallization. Crystals of hCE1 complexes with tamoxifen and benzil were grown using the "dry-drop" method. This protocol involved dissolving the ligand in methanol at a set concentration (1 mM tamoxifen or 10 mM benzil), placing 1 μl of it in the sitting-drop well, and allowing the methanol to evaporate, leaving the dried substance. A protein–mother liquor crystallization drop was then applied to the top of this dehydrated compound. For the hCE1–mevastatin complex, 1 μl of 10 mM mevastatin was added to a drop containing 2 μl of protein plus 2 μl of mother liquor. For the ethyl acetate product complex, 10 mM acetyl-CoA in 5% (v/v) ethanol was added to a drop containing 2 μl of

Table 2. Kinetic data for tamoxifen inhibition

	r^2 for data values using the indicated mode of enzyme inhibition							
Enzyme	General equation	Competitive	Partially competitive	Non-competitive	Partially non-competitive	Mixed	Uncompetitive	K_i (μM)
hCE1	0.987	0.956	0.956	0.956	**0.987**	0.956	0.956	15.2
rCE	0.987	0.923	0.923	0.923	**0.984**	0.923	0.923	23.4

General equation *versus* partially non-competitive equation

	Akaike's information criteria	Favored model	ΔAIC[a]	Probability favored model is correct (%)	Probability general equation is correct (%)	Ratio of probabilities
hCE1	−55.59 *versus* −61.59	Partially non-competitive	−6.00	95.26	4.74	20.09
rCE	−36.53 *versus* −52.21	Partially non-competitive	−15.68	99.06	0.04	2532

General equation: $i = \frac{[I]\{[s](1-\beta)+K_s(\alpha-\beta)\}}{[I]\{[s]+\alpha K_s\}+K_i\{\alpha[s]+\alpha K_s\}}$/. Competitive inhibition, assume $\alpha=\infty$; Partially competitive, assume $1<\alpha<\infty$; $\beta=1$; Non competitive, assume $\alpha=1$; $\beta=0$; Partially non-competitive, assume $\alpha=1$; $0<\beta$ lt;1; Mixed, assume $1<\alpha<\infty$; $\beta=0$; Uncompetitive, assume $\alpha<1$; $\beta<1$.

[a] ΔAIC

protein plus 2 μl of mother liquor. Long, plate-like crystals (up to 800 μm×100 μm×50 μm) were grown by the sitting-drop, vapor-diffusion method at 22 °C in 8–10% (w/v) PEG 3350, 0.1 M citrate (pH 5.5), 0.3 M Li_2SO_4, 0.1 M LiCl, 0.1 M NaCl, and 5% (v/v) glycerol in one week (e.g. for the tamoxifen complex) to two months (e.g. for the benzil complex). Crystals were cryo-protected in 40% (w/v) sucrose plus mother liquor before flash-cooling in liquid nitrogen (Table 2).

Structure determination and refinement

Diffraction data were collected at the Advanced Photon Source at Argonne National Laboratory (Argonne, IL) on beam-line 22-ID (SER-CAT), or at the Stanford Synchrotron Radiation Laboratory (Palo Alto, CA) on beam-lines 9-1 and 9-2. Data were indexed and scaled using HKL2000 or using MOSFLM and SCALEPACK. The structures were determined by molecular replacement with AMoRe,[46] using the hCE1–tacrine complex structure (RCSB PDB accession code 1MX1) as a search model. Refinement was accomplished using simulated annealing and torsion angle dynamics in CNS,[30] with the maximum likelihood function target, and included an overall anisotropic *B*-factor and bulk solvent correction. Prior to any refinement, 7% of the data was removed and set aside for cross-validation using the R_{free} statistic. Non-crystallographic symmetry restraints were employed for the first round of refinement for each complex, but removed for all subsequent rounds to allow for each monomer to be refined independently. Model adjustments and manual rebuilding were accomplished using O,[47] and σ_a-weighted electron density maps.[48] Asparagine-linked glycosylation sites, ligands, sulfate groups, water molecules, and ions were added in the final stages of refinement to achieve the *R*-factors given in Table 1. Final structures exhibit good geometry with no Ramachandran outliers using PROCHECK.[49] Figures were constructed using Dino†, Bobscript,[50] Raster3D,[51] POV-RAY‡, and PyMol§.

† www.dino3d.org
‡ www.povray.org
§ http://pymol.sourceforge.net/

Analysis of mevastatin hydrolysis

The interaction of mevastatin with hCE1 was examined by HPLC followed by liquid chromatography and tandem mas spectrometry (LC-MS/MS). Briefly, reactions containing 125 μM drug were incubated for up to 25 days in the presence of hCE1 at 37 °C in 50 mM Hepes (pH 7.4). The reactions were terminated by adding an equal volume of methanol and, following centrifugation, the products were analyzed by reverse-phase HPLC as described.[41] Peaks obtained from the chromatographic analyses were then subjected to LC-MS/MS using a Shimadzu HPLC connected to a PE SCIEX API 365 LC/MS/MS with Turbo Ion Spray and a heated nebulizer. Data were collected using Analyst version 1.4 software (API). Routinely, results obtained for the different drug metabolites were with 0.5 atomic mass unit (AMU) of their calculated value.

Inhibition assays

Inhibition of hCE1 and rCE-mediated hydrolysis of 3 mM *o*-nitrophenyl acetate was performed as described.[52] Briefly, a spectrophotometric assay was employed and inhibitor concentrations ranged from 128 μM to 1 nM. All assays were performed in duplicate and data were analyzed using a multifactorial equation that also assigned the mode of enzyme inhibition.[53] The equation shown below was used to determine the K_i values.

$$i = \frac{[I]\{[s](1-\beta) + K_s(\alpha-\beta)\}}{[I]\{[s] + \alpha K_s\} + K_i\{\alpha[s] + \alpha K_s\}}$$

where i is the fractional inhibition, [I] is inhibitor concentration, [s] is the substrate concentration, α is the change in affinity of substrate for the enzyme, β is the change in rate of the enzyme-substrate (ES) decomposition, K_s is the dissociation constant of the ES complex, and K_i is the inhibitor constant. The equation can be subdivided into six smaller equations that account for the different types of inhibition. Computer analysis gives the best curve fit (r^2) value that indicates the mode of inhibition based on previously defined assumptions. Definitive assignment of the correct mode of enzyme inhibition was determined using Akaike's Information Criteria.[54,55]

Protein Data Bank accession codes

The coordinates and structure factors have been deposited in the RCSB Protein Data Bank with accession codes 1YA8, 1YAH, 1YA4, 1YAJ, for the mevastatin, ethyl acetate, tamoxifen, and benzil complexes, respectively.

Acknowledgements

The authors thank members of the Redinbo laboratory, particularly J. Chrencik, R. Watkins, J. Orans, D. Teotico, E. Ortlund, S. Lujan, S. Noble, G. Carnahan, Y. Xue, and C. Chen, for discussions and experimental assistance. We thank the SER-CAT staff at APS and the staff at SSRL for assistance with data collection. Use of the Advanced Photon Source was supported by the US Department of Energy, Office of Science, Office of Basic Energy Sciences, under contract no. W-31-109-Eng-38. The research was supported, in part, by the N.I.H. grant CA98468, an NIH Cancer Center Core Grant, P30 CA-21765, and by the American Lebanese Syrian Associated Charities.

Supplementary Data

Supplementary data associated with this article can be found, in the online version, at doi:10.1016/j.jmb.2005.07.016

References

1. Williams, F. M. (1985). Clinical significance of esterases in man. *Clin. Pharmacokinet.* **10**, 392–403.
2. Satoh, T. & Hosokawa, M. (1998). The mammalian carboxylesterases: from molecules to functions. *Annu. Rev. Pharmacol. Toxicol.* **38**, 257–288.
3. Redinbo, M. R., Bencharit, S. & Potter, P. M. (2003). Human carboxylesterase 1: from drug metabolism to drug discovery. *Biochem. Soc. Trans.* **31**, 620–624.
4. Zhang, J., Burnell, J. C., Dumaual, N. & Bosron, W. F. (1999). Binding and hydrolysis of meperidine by human liver carboxylesterase hCE-1. *J. Pharmacol. Expt. Ther.* **290**, 314–338.
5. Tang, B. K. & Kalow, W. (1995). Variable activation of lovastatin by hydrolytic enzymes in human plasma and liver. 4. *Eur. J. Clin. Pharmacol.* **47**, 449–451.
6. Kamendulis, L. M., Brzezinski, M. R., Pindel, E. V., Bosron, W. F. & Dean, R. A. (1996). Metabolism of cocaine and heroin is catalyzed by the same human liver carboxylesterases. *J. Pharmacol. Expt. Ther.* **279**, 713–717.
7. Tabata, T., Katoh, M., Tokudome, S., Hosakawa, M., Chiba, K., Nakajima, M. & Yokoi, T. (2004). Bioactivation of capecitabine in human liver: involvement of the cytosolic enzyme on 5′-deoxy-5-fluorocytidine formation. *Drug Metab. Dispo.* **32**, 762–767.
8. Takai, S., Matsuda, A., Usami, Y., Adachi, T., Sugiyama, T., Katagiri, Y. *et al*. (1997). Hydrolytic profile for ester- or amide-linkage by carboxylesterases pI 5.3 and 4.5 from human liver. *Biol. Pharm. Bull.* **20**, 869–873.
9. Brzezinski, M. R., Abraham, T. L., Stone, C. L., Dean, R. A. & Bosron, W. F. (1994). Purification and characterization of a human liver cocaine carboxylesterase that catalyzes the production of benzoylecgonine and the formation of cocaethylene from alcohol and cocaine. *Biochem. Pharmacol.* **48**, 1747–1755.
10. Bourland, J. A., Martin, D. K. & Mayersohn, M. (1997). Carboxylesterase-mediated transesterification of meperidine (Demerol) and methylphenidate (Ritalin) in the presence of [$^2H_6$]ethanol: preliminary *in vitro* findings using a rat liver preparation. *J. Pharm. Sci.* **86**, 1494–1496.
11. Bencharit, S., Morton, C. L., Hyatt, J. L., Kuhn, P., Danks, M. K., Potter, P. M. & Redinbo, M. R. (2003). Crystal structure of human carboxylesterase 1 complexed with the Alzheimer's drug tacrine: from binding promiscuity to selective inhibition. *Chem. Biol.* **10**, 341–349.
12. Bencharit, S., Morton, C. L., Xue, Y., Potter, P. M. & Redinbo, M. R. (2003). Structural basis of heroin and cocaine metabolism by a promiscuous human drug-processing enzyme. *Nature Struct. Biol.* **10**, 349–356.
13. Bencharit, S., Morton, C. L., Howard-Williams, E. L., Danks, M. K., Potter, P. M. & Redinbo, M. R. (2002). Structural insights into CPT-11 activation by mammalian carboxylesterases. *Nature Struct. Biol.* **9**, 337–432.
14. Evans, M., Roberts, A., Davies, S. & Rees, A. (2004). Medical lipid-regulating therapy: current evidence, ongoing trials and future developments. *Drugs*, **64**, 1181–1196.
15. Mauro, V. F. & MacDonald, J. L. (1991). Simvastatin: a review of its pharmacology and clinical use. *DICP*, **25**, 257–264.
16. Istvan, E. S. & Deisenhofer, J. (2001). Structural mechanism for statin inhibition of HMG-CoA reductase. *Science*, **292**, 1160–1164.
17. Buzdar, A. U. (2000). Tamoxifen's clinical applications: old and new. *Arch. Fam. Med.* **9**, 906–912.
18. Jones, K. L. & Buzdar, A. U. (2004). A review of adjuvant hormonal therapy in breast cancer. *Endocr. Relat. Cancer*, **11**, 391–406.
19. Etienne, M. C., Milano, G., Fischel, J. L., Frenay, M., Francois, E., Formento, J. L. *et al*. (1989). Tamoxifen metabolism: pharmacokinetic and *in vitro* study. *Br. J. Cancer*, **60**, 30–35.
20. Mesange, F., Sebbar, M., Capdevielle, J., Guillemot, J. C., Ferrara, P., Bayard, F. *et al*. (2002). Identification of two tamoxifen target proteins by photolabeling with 4-(2-morpholinoethoxy)benzophenone. *Bioconjug. Chem.* **13**, 766–772.
21. Morello, K. C., Wurz, G. T. & DeGregorio, M. W. (2002). SERMs: current status and future trends. *Crit. Rev. Oncol. Hematol.* **43**, 63–76.
22. Becker, A., Bottcher, A., Lackner, K. J., Fehringer, P., Notka, F., Aslanidis, C. & Schmitz, G. (1994). Purification, cloning, and expression of a human enzyme with acyl coenzyme a: cholesterol acyltransferase activity, which is identical to liver carboxylesterase. *Arterioscler. Thromb.* **14**, 1346–1355.
23. Ghosh, S. (2000). Cholesteryl ester hydrolase in human monocyte/macrophage: cloning, sequencing, and expression of full-length cDNA. *Physiol. Genomics*, **2**, 1–8.
24. Diczfalusy, M. A., Bjorkhem, I., Einarsson, C., Hillebrant, C. G. & Alexson, S. E. (2001). Characterization of enzymes involved in formation of ethyl esters of long-chain fatty acids in humans. *J. Lipid Res.* **42**, 1025–1032.
25. Beckemeier, M. E. & Bora, P. S. (1998). Fatty acid ethyl esters: potentially toxic products of myocardial ethanol metabolism. *J. Mol. Cell. Cardiol.* **30**, 2487–2494.

26. Lange, L. G. & Sobel, B. E. (1983). Mitochondrial dysfunction induced by fatty acid ethyl esters, myocardial metabolites of ethanol. *J. Clin. Invest.* **72**, 724–731.
27. Bora, P. S., Farrar, M. A., Miller, D. D., Chaitman, B. R. & Guruge, B. L. (1996). Myocardial cell damage by fatty acid ethyl esters. *J. Cardiovasc. Pharmacol.* **27**, 1–6.
28. Bora, P. S., Guruge, B. L., Miller, D. D., Chaitman, B. R. & Ruyle, M. S. (1996). Purification and characterization of human heart fatty acid ethyl ester synthase/carboxylesterase. *J. Mol. Cell. Cardiol.* **28**, 2027–2032.
29. Wadkins, R. M., Hyatt, J. L., Wei, X., Yoon, K. J., Wierdl, M., Edwards, C. C. *et al*. (2005). Identification and characterization of novel benzil (diphenylethane-1,2-dione) analogues as inhibitors of mammalian carboxylesterases. *J. Med. Chem.* **48**, 2906–2915.
30. Brunger, A. T., Adams, P. D., Clore, G. M., DeLano, W. L., Gros, P., Grosse-Kunstleve, R. W. *et al*. (1998). Crystallography & NMR system: a new software suite for macromolecular structure determination. *Acta Crystallog. sect. D*, **54**, 905–921.
31. Thompson, J. D., Higgins, D. G. & Gibson, T. J. (1994). CLUSTAL W: improving the sensitivity of progressive multiple sequence alignment through sequence weighting, position-specific gap penalties and weight matrix choice. *Nucl. Acids Res.* **22**, 4673–4680.
32. Kaphalia, B. S. & Ansari, G. A. (2001). Purification and characterization of rat hepatic microsomal low molecular weight fatty acid ethyl ester synthase and its relationship to carboxylesterases. *J. Biochem. Mol. Toxicol.* **15**, 165–171.
33. Hosokawa, M., Maki, T. & Satoh, T. (1987). Multiplicity and regulation of hepatic microsomal carboxylesterases in rats. *Mol. Pharmacol.* **31**, 579–584.
34. Musidlowska-Persson, A. & Bornscheuer, U. T. (2003). Recombinant porcine intestinal carboxylesterase: cloning from the pig liver esterase gene by site-directed mutagenesis, functional expression and characterization. *Protein Eng.* **16**, 1139–1145.
35. Corsini, A., Maggi, F. M. & Catapano, A. L. (1995). Pharmacology of competitive inhibitors of HMG-CoA reductase. *Pharmacol. Res.* **31**, 9–27.
36. Brown, M. S., Faust, J. R. & Goldstein, J. L. (1978). Induction of 3-hydroxy-3-methylglutaryl coenzyme A reductase activity in human fibroblasts incubated with compactin (ML-236B), a competitive inhibitor of the reductase. *J. Biol. Chem.* **253**, 1121–1128.
37. Chakravarti, R. & Sahai, V. (2004). Compactin—a review. *Appl. Microbiol. Biotechnol.* **64**, 618–624.
38. Endo, A., Kuroda, M. & Tanzawa, K. (1976). Competitive inhibition of 3-hydroxy-3-methylglutaryl coenzyme A reductase by ML-236A and ML-236B fungal metabolites, having hypocholesterolemic activity. *FEBS Letters*, **72**, 323–326.
39. Darvesh, S., Martin, E., Walsh, R. & Rockwood, K. (2004). Differential effects of lipid-lowering agents on human cholinesterases. *Clin. Biochem.* **37**, 42–49.
40. Williams, P. A., Cosme, J., Vinkovic, D. M., Ward, A., Angove, H. C., Day, P. J. *et al*. (2004). Crystal structures of human cytochrome P450 3A4 bound to metyrapone and progesterone. *Science*, **305**, 683–686.
41. Billecke, S., Draganov, D., Counsell, R., Stetson, P., Watson, C., Hsu, C. & La Du, B. N. (2000). Human serum paraoxonase (PON1) isozymes Q and R hydrolyze lactones and cyclic carbonate esters. *Drug Metab. Dispos.* **28**, 1335–1342.
42. Kusama, M., Miyauchi, K., Aoyama, H., Sano, M., Kimura, M., Mitsuyama, S. *et al*. (2004). Effects of toremifene (TOR) and tamoxifen (TAM) on serum lipids in postmenopausal patients with breast cancer. *Breast Cancer Res. Treat.* **88**, 1–8.
43. Barry, M., Mulcahy, F., Merry, C., Gibbons, S. & Back, D. (1999). Pharmacokinetics and potential interactions amongst antiretroviral agents used to treat patients with HIV infection. *Clin. Pharmacokinet.* **36**, 289–304.
44. Danks, M. K., Morton, C. L., Krull, E. J., Cheshire, P. J., Richmond, L. B., Naeve, C. W. *et al*. (1999). Comparison of activation of CPT-11 by rabbit and human carboxylesterases for use in enzyme/prodrug therapy. *Clin. Cancer Re.* **5**, 917–924.
45. Morton, C. L. & Potter, P. M. (2000). Comparison of *Escherichia coli, Saccharomyces cerevisiae, Pichia pastoris, Spodoptera frugiperda*, and COS7 cells for recombinant gene expression. Application to a rabbit liver carboxylesterase. *Mol. Biotechnol.* **16**, 193–202.
46. Navaza, J. (1994). AmoRe: an automated package for molecular replacement. *Acta Crystallog. sect. A*, **50**, 157–163.
47. Jones, T. A., Zou, J. Y., Cowan, S. W. & Kjeldgaard, M. (1991). Improved methods for building protein models in electron density maps and the location of errors in these models. *Acta Crystallog. sect. A*, **47**, 110–119.
48. Read, R. J. (1986). Improved Fourier Coefficients for maps using phases from partial structures with errors. *Acta Crystallog. sect. A*, **42**, 140–149.
49. Laskowski, R. A., MacArthur, M. W., Moss, D. S. & Thornton, J. M. (1993). PROCHECK: a program to check the stereochemical quality of protein structures. *J. Appl. Crystallog.* **26**, 283–291.
50. Esnouf, R. M. (1999). Further additions to MolScript version 1.4, including reading and contouring of electron-density maps. *Acta Crystallog. sect. D*, **55**, 938–940.
51. Merritt, E. A. & Murphy, M. E. P. (1994). Raster3D version 2.0. A program for photorealistic molecular graphics. *Acta Crystallog. sect. D*, **50**, 869–873.
52. Wadkins, R. M., Hyatt, J. L., Yoon, K. J., Morton, C. L., Lee, R. E., Damodaran, K. *et al*. (2004). Discovery of novel selective inhibitors of human intestinal carboxylesterase for the amelioration of irinotecan-induced diarrhea: synthesis, quantitative structure-activity relationship analysis, and biological activity. *Mol. Pharmaco.* **65**, 1336–1343.
53. Webb, J. L. (1963). *Enzyme and Metabolic Inhibitors General Principles of Inhibition*, vol. 1, Academic Press Inc, New York, NY.
54. Akaike, H. (1973). *Information theory and an extension of the maximum likelihood principle Second International Symposium on Information Theory,* Akademiai kiado, Budapest.
55. Akaike, H. (1974). A new look at the statistical model indentification. *IEEE Trans. Automatic Control*, **AC-19**, 716–723.

Edited by I. Wilson

(Received 4 January 2005; received in revised form 5 July 2005; accepted 6 July 2005)
Available online 25 July 2005